SUPPLEMENTAL MATERIAL

Detailed Methods

Human CPCs

As previously described, samples of human myocardium discarded at surgery (n = 6) were utilized to isolate, expand and characterize c-kit-positive human cardiac progenitor cells (hCPCs) (1). Briefly, specimens were enzymatically dissociated in a solution containing collagenase to obtain a single cell suspension (1). Cells were sorted with magnetic immunobeads for c-kit (Miltenyi) and the cell phenotype was defined by immunolabeling (1). Human CPCs were then cultured in F12 medium (Gibco) supplemented with 5-10% FBS (Gibco) and insulin-selenium-transferrin mixture (Sigma). At P3-P6, cells were characterized by FACS to document their undifferentiated state (1). Cells were fixed in 4% paraformaldehyde for 15 min and tested for markers of cardiac and hematopoietic cell lineages (1, 2).

Cell Cycle Synchronization

hCPCs were incubated for 24 h with mimosine (synchronization at G1-S transition, 500 μmol/L; Sigma) or demecolcine (synchronization at G2-M transition, 20 ng/ml; Sigma) (3, 4). Subsequently, cells were suspended, washed in PBS and fixed in ice-cold ethanol (70%) for 2 h. Nuclei were stained by propidium iodide (20μg/ml; Sigma), Triton X-100 (0.1%; Sigma) and RNase A (10mg/ml; Sigma) for 1 h. The distribution of non-synchronized and synchronized hCPCs in the cell cycle was determined by fluorescence activated cell sorting (BD FACS Aria High Speed Sorter SORP System™) and the percentage of cells in G1, S and G2 was determined by ModFit LT™ software. Additionally, non-synchronized control hCPCs and hCPCs treated with mimosine and demecolcine were analyzed physiologically.

Ca^{2+} Oscillations in hCPCs

hCPCs were loaded with 10 μmol/L Fluo-3 AM (Invitrogen) and placed on the stage of a two-photon microscope (BX51WI Olympus microscope coupled with a Bio-Rad Radiance 2100MP system). Cells were bathed with a Tyrode solution containing (mmol/L): NaCl 140, KCl 5.4, $MgCl_2$ 1, HEPES 5, Glucose 5.5 and $CaCl_2$ 2.0 (pH 7.4, adjusted with NaOH). Fluo-3 was excited at 900-960 nm wavelength with mode-locked Ti:sapphire femtosecond laser (Tsunami, Spectra-Physics) and the emission signal was collected at 535 nm. Series of images were acquired at 10 sec intervals for a period of 33 min. Changes of intracellular Ca^{2+} in individual hCPCs were determined by measuring the fluorescent signal of Fluo-3. In each cell, the oscillations in fluorescence with time were graphically visualized utilizing ImageJ and

Microsoft Office Excel. These traces were employed to assess the number, amplitude and duration of Ca^{2+} oscillations in hCPCs. Fluo-3 signals were expressed as normalized fluorescence (F/F_0). The duration of Ca^{2+} oscillations was measured from the onset of the rising phase to the return to baseline.

The effects of hCPC coupling and uncoupling on Ca^{2+} oscillations (5, 6) were determined in the presence of the connexin hemi-gap junction channel blocker octanol (1 mmol/L; Sigma). Additionally, thimerosal (10 μmol/L, Sigma) was utilized to enhance the affinity of IP3Rs to IP3 (4, 7); IP3R function was inhibited (5, 9, 9) with 2-APB (2-aminoethyl diphenylborinate, 75 μmol/L; Sigma) and xestospongin-C (10 μmol/L; Sigma) and SERCA (10, 11) with CPA (cyclopiazonic acid, 10 μmol/L; Sigma). PLC activity was attenuated (12, 13) with U-73122 (2 μmol/L; Sigma) while caffeine (10 mmol/L; Sigma) and ryanodine (10 μmol/L; MP Biomedicals) were used to modulate RyR channels (4, 14-16). Purinoreceptors, H1 receptors and IGF-1R were activated with ATP (10 μmol/L; Sigma), histamine (100 μmol/L; Sigma), and IGF-1 (200 ng/ml; PeproTech), respectively. Finally, thapsigargin (10 μmol/L; Sigma) was introduced to deplete ER Ca^{2+} stores (11), lanthanum (0.1 mmol/L; Sigma) and SKF-96365 (0.1 mmol/L; Sigma) to block SOC (11, 17, 18, 19), KB-R7943 (100 μmol/L; Tocris) to inhibit forward mode NCX (20, 21) and carboxyeosin (5 μmol/L; Sigma) to prevent PMCA function (21, 22).

In co-culture experiments, hCPCs were plated with rat neonatal ventricular myocytes (purity: >90%) and were labeled with 1-2 μmol/L red fluorescent dye 1,1'-dilinoleyl-3,3,3',3'-tetramethylindocarbocyanine (DiI, Invitrogen) for 5 min at 37°C and then for 15 min at room temperature (1, 23, 24). Fluo-3 loaded myocytes (1, 24) and DiI labeled hCPCs were analyzed by series of images (5 sec sampling rate) or by line-scan mode (2 ms sampling rate) (1, 24). Cells were field stimulated with platinum electrodes utilizing a Grass S88 stimulator (Astro-Med Industrial Park) in the absence and presence of 0.2 mmol/L cadmium chloride to inhibit I_{CaL} (1, 2, 14, 16, 24).

Dye Transfer Assay

hCPCs were microinjected (FemtoJet, Eppendorf AG) with a medium containing in mmol/L: 27 K_2HPO_4, 8 $NaHPO_4$, 26 KH_2PO_4, 1 mg/ml cascade blue (Invitrogen) and 0.3 mg/ml of the high-molecular-mass (70,000) rhodamine-labeled dextran (Invitrogen) (24, 25, 26). Transfer of the fluorescent dye to neighboring cells was followed by acquisition of subsequent images using an inverted epifluorescence microscope (IX-71, Olympus). This analysis was performed in 5 independent preparations.

In a second assay, cell-to-cell coupling was assessed by co-culture of calcein loaded hCPCs with non-loaded hCPCs or neonatal myocytes. hCPCs were labeled with 1-2 μmol/L DiI and loaded with 5 μmol/L calcein-acetoxymethyl ester (Invitrogen) prior to co-culture. Since DiI is incorporated permanently into the cell membrane, the presence of green fluorescence in DiI-negative cells was considered indicative of the transfer of calcein from loaded hCPCs to non-loaded cells via functional gap junctions. This analysis was performed by two photon microscopy (1, 23, 24). Nuclei in living cells were labeled with 10 μM Hoescht 33258 dye (Sigma) (15). Images were acquired and utilized to measure by ImageJ software the level of fluorescence of calcein in DiI-positive hCPCs and neighboring and distant DiI-negative cells.

Mouse Myocytes and CPCs

All animal experiments were approved by the local animal care committee (IACUC). C57BL/6 mice (Jackson Laboratory) and transgenic mice expressing EGFP under the control of the c-kit promoter (c-kit-EGFP mouse) (27) or under the control of the α-myosin heavy chain promoter (MHC-EGFP mouse) (24) were anesthetized with sodium pentobarbital (50 mg/kg body weight, i.p.), the heart was excised and cardiac cells were enzymatically dissociated (14, 16, 24, 28). Briefly, the myocardium was perfused retrogradely through the aorta at 37°C with a Ca^{2+}-free solution gassed with 85% O_2 and 15% N_2. After 5 minutes, 0.1 mmol/L $CaCl_2$, 274 units/ml collagenase (type 2, Worthington Biochemical Corp) and 0.57 units/ml protease (Type XIV, Sigma) were added to the solution which contained in mmol/L: NaCl 126, KCl 4.4, $MgCl_2$ 5, HEPES 5, Glucose 22, Taurine 20, Creatine 5, Na Pyruvate 5 and NaH_2PO_4 5 (pH 7.4). At completion of digestion, the left ventricular (LV) myocardium was cut in small pieces and re-suspended in Ca^{2+} 0.1 mmol/L solution and myocytes and small cells were collected separately. LV myocytes from C57BL/6 mice were utilized for measurement of L-type Ca^{2+} current (14, 16, 24, 28). Cardiomyocytes from transgenic MHC-EGFP mice were loaded with the Ca^{2+} indicator Rhod-2 (10 μM; Invitrogen) and emission spectra for EGFP and Rhod-2 were analyzed by Zeiss LSM 510 META confocal microscope. Moreover, myocytes were bathed with a Tyrode solution and electrically stimulated. Ca^{2+} transients were acquired by two-photon microscopy working in line-scan mode (1, 24). EGFP and Rhod-2 fluorescent signals were collected simultaneously. Small cells from the heart of transgenic c-kit-EGFP mice were FACS sorted for EGFP. For Ca^{2+} imaging, EGFP-positive CPCs were cultured in a medium containing F12 Kaighn's medium (Gibco) supplemented with 10% FBS (Gibco), bFGF (PeproTech) and LIF (Millipore) (2).

Ex Vivo Preparation

For the analysis of intracellular Ca^{2+} in myocytes and CPCs in situ within the myocardium, c-kit-EGFP mice (n = 6) were employed (27). Animals were anesthetized with sodium pentobarbital (50 mg/kg body weight, i.p.), and the heart was excised and perfused retrogradely through the aorta with an oxygenated Tyrode solution containing the Ca^{2+} indicator Rhod-2 (10 μM; Invitrogen). Subsequently, the heart was continuously perfused and superfused with an oxygenated Tyrode solution containing cytochalasin D (50 mmol/L; Sigma) to inhibit contraction (1, 24) and placed in a bath mounted on the stage of a two-photon microscope working in line-scan mode. Electrical stimulation was accomplished by depolarizing pulses. The red fluorescence of Rhod-2 was detected in EGFP-positive CPCs and EGFP-negative myocytes.

Patch-clamp

Data were acquired by means of the whole-cell patch-clamp technique in voltage-clamp mode using a Multiclamp 700A amplifier (Axon Instruments). Electrical signals were digitized using a 500 kHz 16-bit resolution A/D converter (Digidata 1322, Axon Instruments) and recorded using pCLAMP 9.0 software (Axon Instruments) with low-pass filtering at 2 kHz (14, 16, 24, 28, 29). Cells were bathed with Tyrode solution containing 1 mmol/L $CaCl_2$. Composition of the pipette solution in mmol/L: NaCl 10, KCl 113, $MgCl_2$ 0.5, K_2-ATP 5, Glucose 5.5, EGTA 5, HEPES 10 (pH 7.2). The pipettes were pulled by means of a glass microelectrode puller (PB-7, Narishige) and when filled had a resistance of 1-3 MΩ. Current-voltage (I-V) relation for I_{CaL} was determined applying depolarizing steps 1 sec in duration from holding potential (V_h) -50 mV in 10 mV increments. I_{CaL} amplitude was measured as the difference between the peak inward current at the beginning of the step and the current at the end of the 1 sec step (14, 16, 28). Membrane capacitance (C_m) was calculated using a 5 mV voltage step and utilized to normalize current recordings (14, 16, 28).

Proliferation, Apoptosis and Differentiation Assays

Proliferation of hCPCs was determined by BrdUrd incorporation (30) while apoptosis was evaluated by Annexin V labeling and flow cytometry. Cells were starved for a 24 h period and then were incubated for 30 min in 200 ng/ml IGF-1 (PeproTech), 100 μmol/L ATP (Sigma), 100 μmol/L histamine (Sigma), 75 μmol/L 2-APB (Sigma), 1 μmol/L U-73122 (Sigma), or 10 μmol/L xestospongin-C (Sigma). After washing with PBS, hCPCs were exposed for an additional 24 h to serum-free medium. For proliferation assay, BrdUrd (1 μg/ml; Roche) was added twice, at the beginning of the experiment and 23 h later. At completion, cells were fixed for 20 min at -20º C in a glycine buffer/70% ethanol. BrdUrd incorporation

was determined by immunostaining with monoclonal antibody (Roche). For apoptosis, cells were labeled with Annexin V (Invitrogen) and analyzed by FACS (FACSAria, Becton Dickinson). hCPC differentiation was induced by MEM containing 10% FBS and 10^{-8} mol/L dexamethasone (Sigma) (1, 2). The effects of Ca^{2+} oscillations on the commitment of hCPCs to the myocyte lineage was tested by adding 100 μmol/L ATP or 100 μmol/L histamine to the culture media every 48 h. Cultured cells were analyzed after 1 week by immucytochemistry.

Phospholipase C-β3 siRNA

For siRNA experiments, ON-TARGET plus siRNA pool (Fisher Scientific) against human PLC-β3 was transfected to hCPCs at the final concentration of 50 nmol/L with N-TER Nanoparticle siRNA Transfection System (Sigma) according to manufacturer instructions. Non-targeting siRNA pool (Fisher Scientific) was utilized for the transfection of control hCPCs. Transfection solution was replaced with the normal medium after 24 h. Transcript levels for PLC-β3 hCPCs were analyzed 3 days after transfection.

Myocardial Infarction and Cell Implantation

Under ketamine (120 mg/kg body weight, i.p.) and xylazine (0.5 mg/kg body weight, i.p.) anesthesia, myocardial infarction was produced in female C57BL/6 mice at 12 weeks of age utilizing a protocol previously described (1, 24, 31). Shortly thereafter, 60,000 EGFP-positive hCPCs, suspended in 10 μl PBS in the presence of 1% rhodamine labeled polystyrene microspheres (Invitrogen), were injected in the myocardium in four sites bordering the infarct. Cell tagging was achieved by infecting hCPCs with a lentivirus expressing EGFP under the control of the cytomegalovirus promoter (LentiV-CAG-GFP) (1). Prior to implantation, hCPCs were serum-starved for 24 h followed by 30 min exposure to ATP (100 μmol/L) or histamine (100 μmol/L). Control cells were kept in serum-free medium only. Untreated mice received injections of PBS. To recognize newly formed cells, mice were treated with BrdUrd (50 mg/kg body weight, i.p., every 12 h) (1, 2, 16, 23, 24, 31). Immunosuppresive regimen consisted of cyclosporine A (Sigma), 50 mg/kg body weight, i.p. daily (1). Mice were sacrificed 48 h and 7 days after hCPC implantation. In a subset of mice, left ventricular hemodynamics (1, 14, 24, 28, 31) was obtained in the closed chest preparation with a MPVS-400 system for small animals (Millar Instruments) equipped with a PVR-1045 catheter. Under sodium pentobarbital (50 mg/kg body weight, i.p.) anesthesia, the right carotid artery was exposed and the pressure transducer was inserted in the carotid artery and advanced in the LV cavity. Data were acquired and analyzed with Chart 5 (ADInstruments) and PVAN softwares. The heart was arrested in diastole and fixed by perfusion with phosphate buffered formalin (1, 2, 14, 23, 24, 31).

For animals sacrificed at 48 h, two transverse sections of the LV which included the sites of injections were obtained for immunolabeling studies. The sites of cell delivery were identified by the presence of rhodamine labeled microspheres. For mice sacrificed at 7 days, base, mid-portion and apex of the LV were processed. Tissue sections 4 μm in thickness were used for immunohistochemistry and were analyzed by epifluorescence (BX51 Olympus microscope) and confocal (IX71 Olympus inverted microscope coupled with a Bio-Rad Radiance 2100 system) microscopy.

To determine the number of EGFP-positive cells in the myocardium (N) the volume occupied by the injected cells (V) was computed assuming an ellipsoid configuration. The volume of EGFP-positive cells (V_C) was determined by confocal microscopy. The quotient of these two values yielded the number of engrafted cells:

$$N = V / V_C$$

To determine whether myocardial infarction enhanced the number of c-kit-positive EGFP-positive cells in the heart of c-kit-EGFP transgenic mice, permanent coronary artery occlusion was performed. Animals were sacrificed 48 hours later.

Immunocytochemistry

Formalin-fixed tissue sections, 4 μm in thickness, and paraformaldehyde-fixed cultured hCPCs and myocytes were studied. The antibodies employed and the labeling protocols are listed in Supplemental Table 7. Nuclei were stained by DAPI (Sigma).

Quantitative RT-PCR

RNA was extracted from cultured hCPCs utilizing TRI REAGENT (Sigma) as described previously (1, 16, 24, 30). Human heart total RNA (Applied Biosystems) was utilized as control. cDNA was obtained from 2 μg total RNA in a 20 μl reaction containing Reverse Transcription buffer (Applied Biosystems), 1 mmol/L each of dTTP, dATP, dGTP and dCTP together with 50 U of MultiScribe reverse transcriptase (Applied Biosystems), 20 U of RNase inhibitor (Applied Biosystems) and 100 pmole of oligo-$(dT)_{15}$ primer. This mixture was incubated at 37°C for 2 h. Subsequently, real-time RT-PCR was performed with primers (Supplemental Table 8) designed using the Vector NTI Advance 10 software (Invitrogen). The 7300 Real Time PCR system (Applied Biosystems) was employed for quantitative RT-PCR. In each case, 1 μl of cDNA was combined with Power SYBR Green Master Mix (Applied Biosystems) in a 25 μl reaction. Cycling conditions were as follow: 95°C for 10 min followed by 40 cycles of amplification (95°C denaturation for 15 sec, 60°C annealing and extension for 1 min). The melting curve was then

obtained. To avoid the influence of genomic contamination, forward and reverse primers for each gene were located in different exons. PCR products were run on 2% agarose/1x TAE gel to confirm the specificity of the reaction.

Statistical Analysis

The number of experiments performed in each assay (n) has been included in Supplemental Tables 1-5. Data are presented as mean±SEM and statistical significance was determined by two-tailed unpaired Student's *t* test and the analysis of variance and Bonferroni method (32, 33). *P* values of less than < 0.05 were considered to be significant.

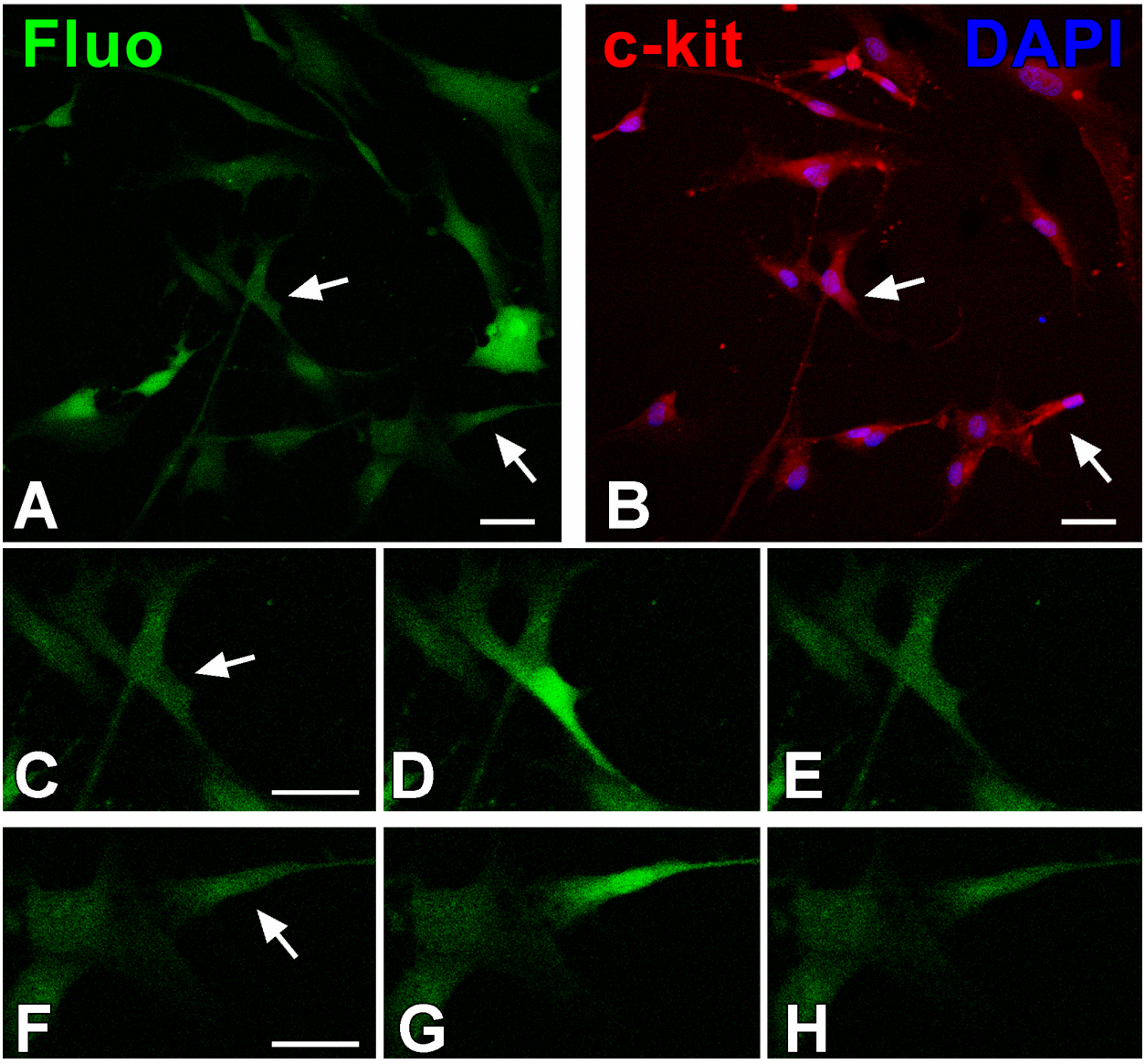

Figure I. Intracellular Ca^{2+} in c-kit-positive hCPCs. **A-H**, hCPCs loaded with the Ca^{2+} sensitive dye Fluo-3 (Fluo, green) (**A**) were monitored for intracellular Ca^{2+} oscillations and subsequently fixed and stained (**B**) with DAPI (blue) and c-kit antibody (red). The c-kit receptor was detected in cells (arrows) experiencing Ca^{2+} oscillations (**C-E** and **F-H**). Scale bars: 40 μm.

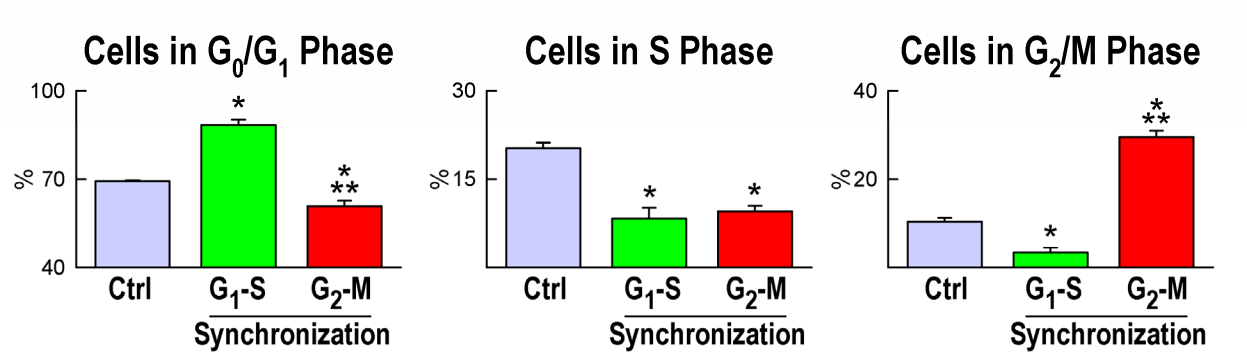

Figure II. Synchronization of hCPCs. hCPCs in G_0/G_1, S and G_2/M in control condition (Ctrl, n=10) and at G_1-S (G_1-S, n=7) and G_2-M phase with demecolcine (G_2-M, n=6).

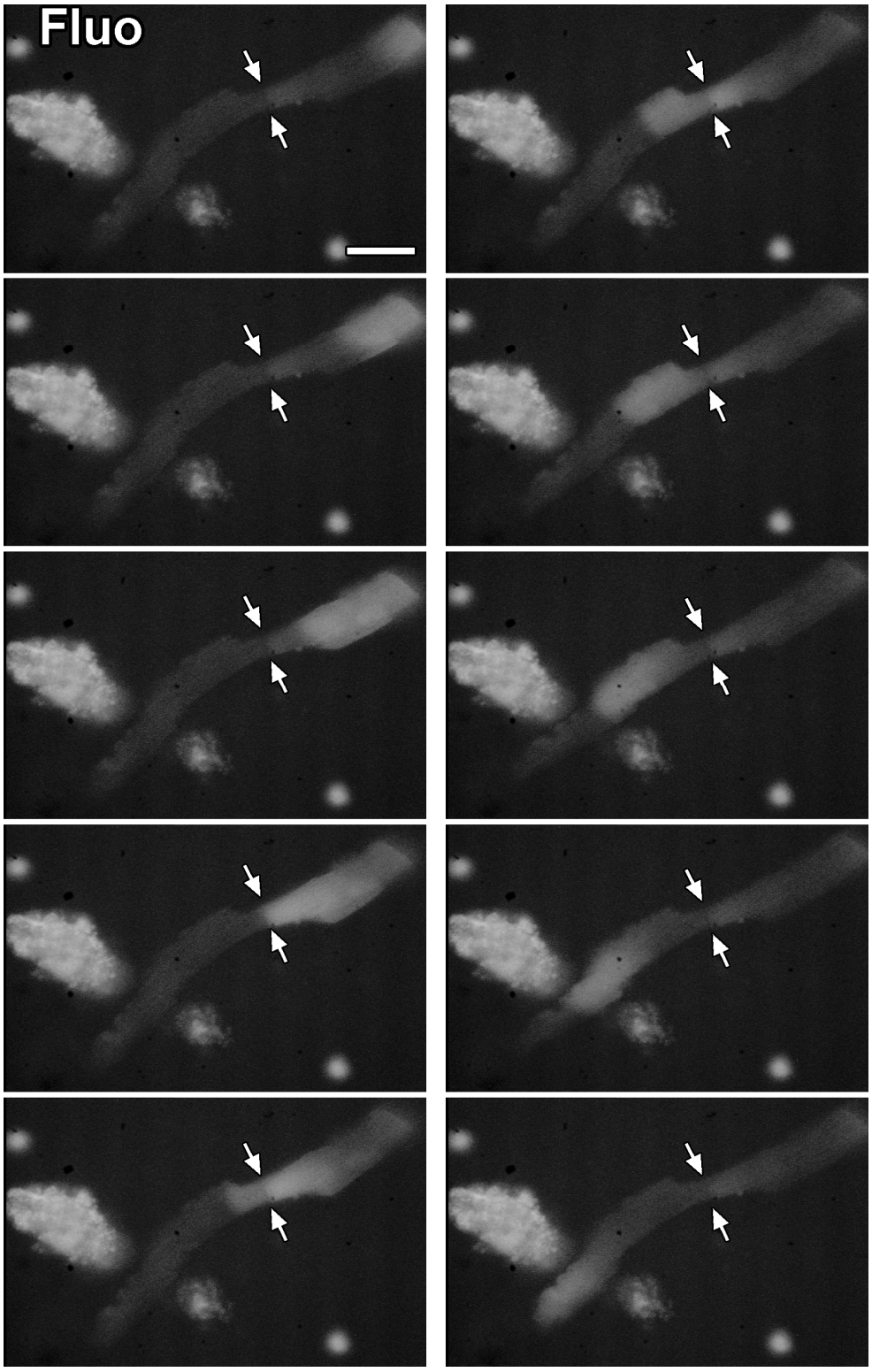

Figure III. Propagation of a Ca^{2+} wave in a myocyte doublet loaded with Fluo-3. Arrowheads indicate the interface between the two myocytes. Scale bar, 50 μm. Images were obtained from Supplemental Movie 1.

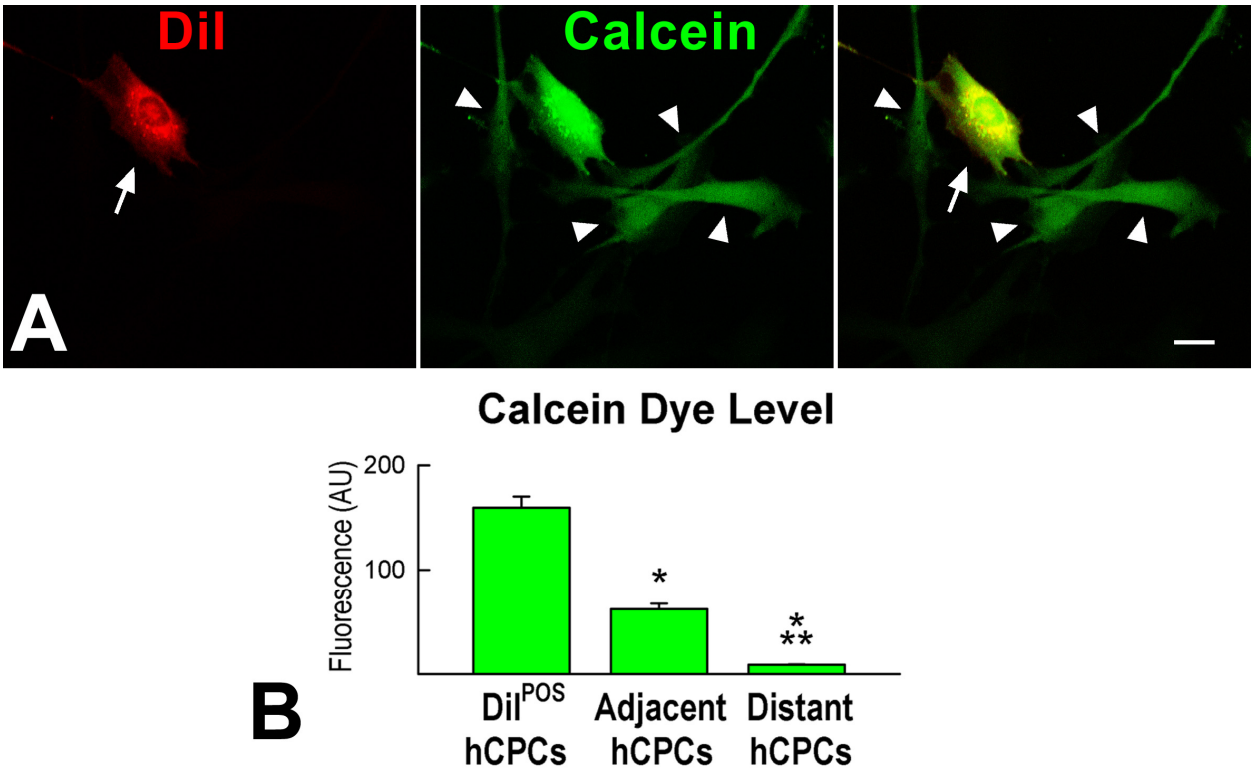

Figure IV. Cell-to-cell interaction. **A**, hCPC (arrow) labeled by both DiI (left panel, red) and calcein (central panel, green). Calcein is transferred form the labeled hCPC to adjacent DiI-negative hCPCs (arrowheads, green). The merge of the two dyes is shown in the right panel. Scale bar: 20 μm. **B**, Calcein fluorescence in DiI-positive (DiI^{POS}) and adjacent and distant DiI-negative hCPCs.

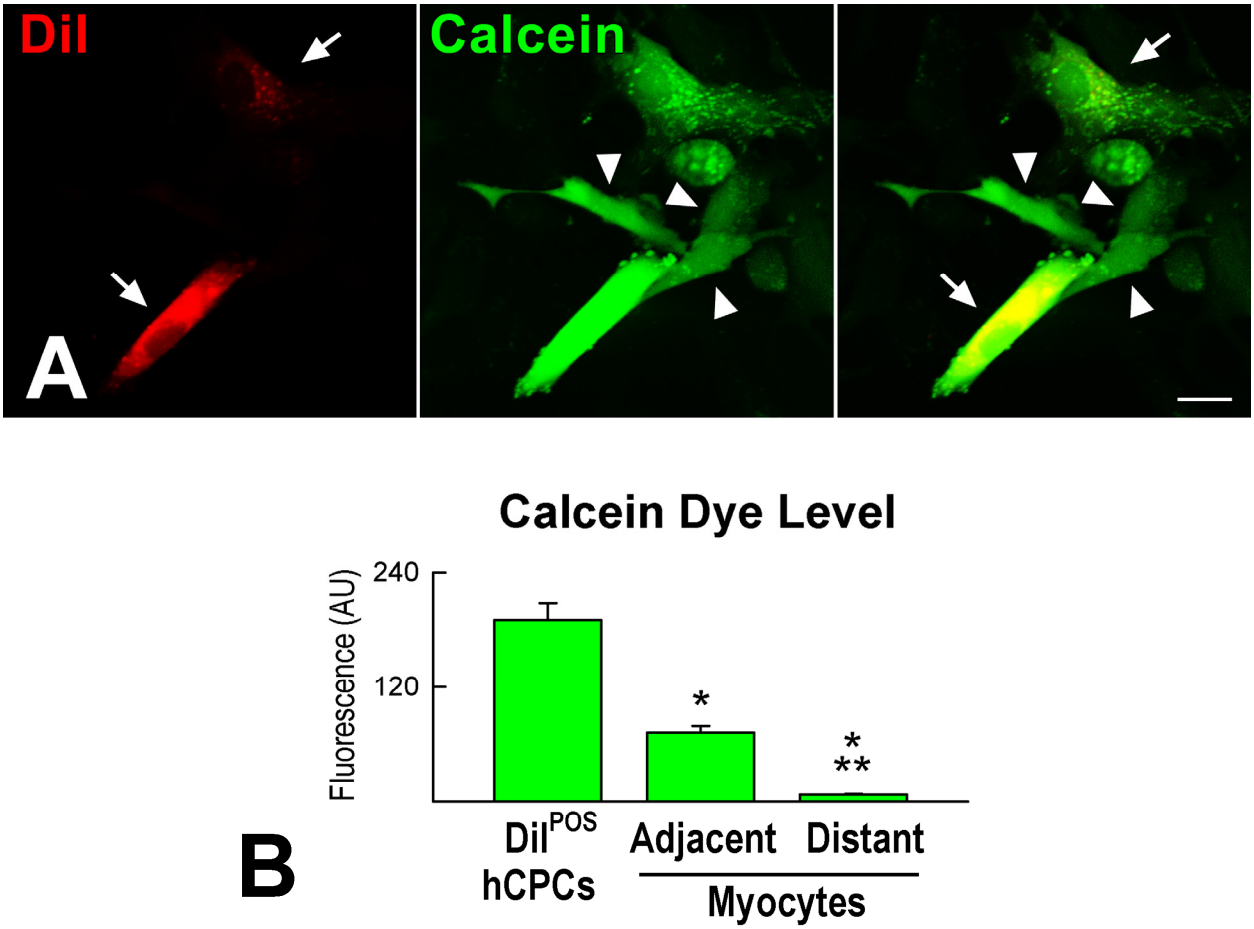

Figure V. Cell-to-cell interaction between hCPCs and myocytes. **A**, hCPCs (arrows) labeled by both DiI (left panel, red) and calcein (central panel, green). Calcein is transferred form labeled hCPCs to adjacent DiI-negative neonatal myocytes (arrowheads, green). The merge of the two dyes is shown in the right panel. Scale bar: 20 μm. **B**, Calcein fluorescence in DiI-positive (DiI^{POS}) and adjacent and distant DiI-negative myocytes.

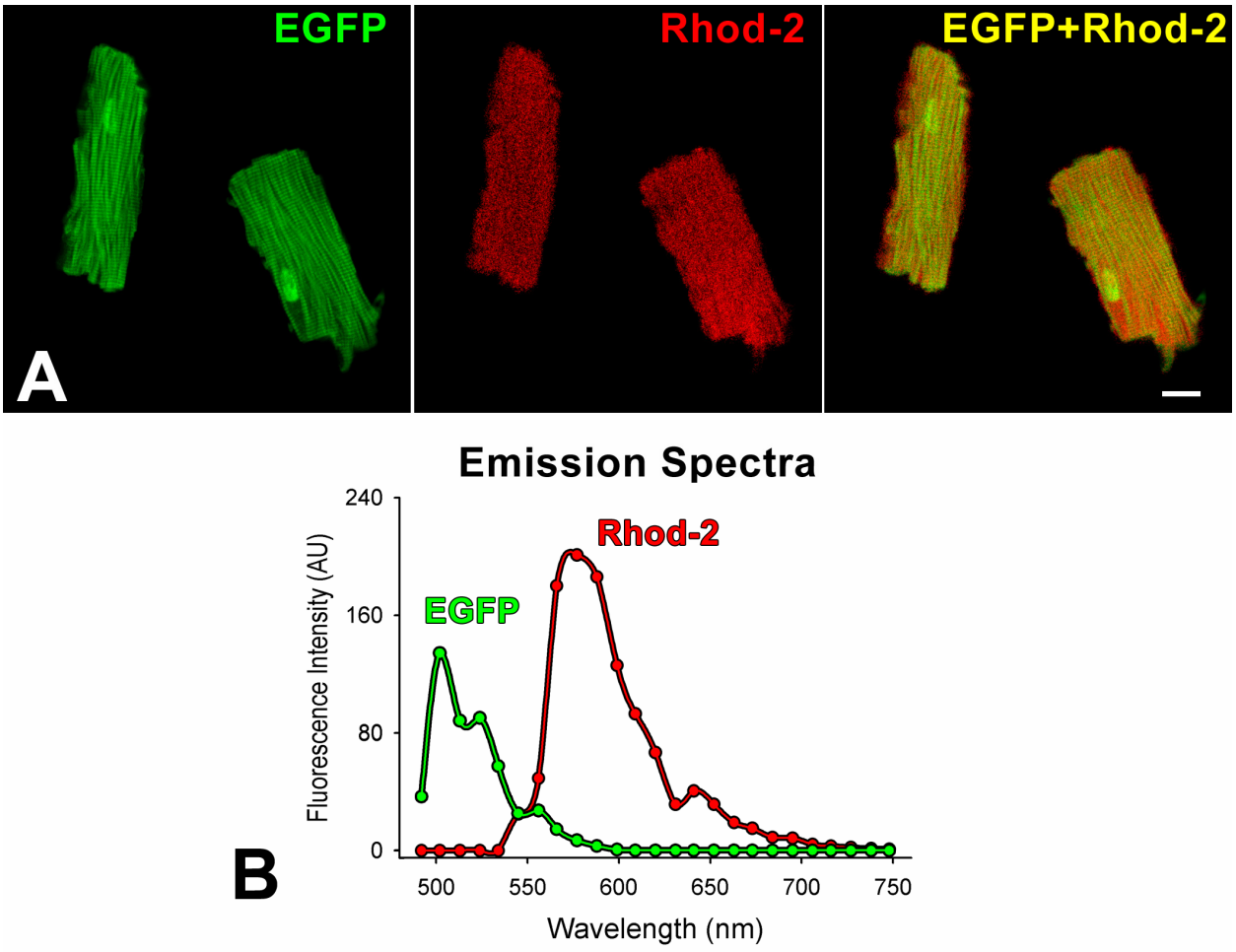

Figure VI. Intracellular Ca^{2+} in EGFP positive cells. **A**, Cardiomyocytes isolated from transgenic mice in which EGFP is expressed under the control of the α-myosin heavy chain promoter (MHC-EGFP). Myocytes were loaded with the calcium indicator Rhod-2 and fluorescent signals of the two molecules were examined by spectral analysis. **B**, EGFP and Rhod-2 show separate emission spectra. **C-K**, Myocyte isolated from a MHC-EGFP mouse heart (C, F, I). Following electrical stimulation, EGFP and Rhod-2 signals were acquired and are illustrated together (D) and separately (G and J). The corresponding traces are shown in the lower part of each panel (E, H, K). Ca^{2+} transients were obtained in 20 myocytes isolated from 2 transgenic mice. EGFP had minimal, if any, effect on the ability to measure Ca^{2+} transients. Scale bars: 20 μm.

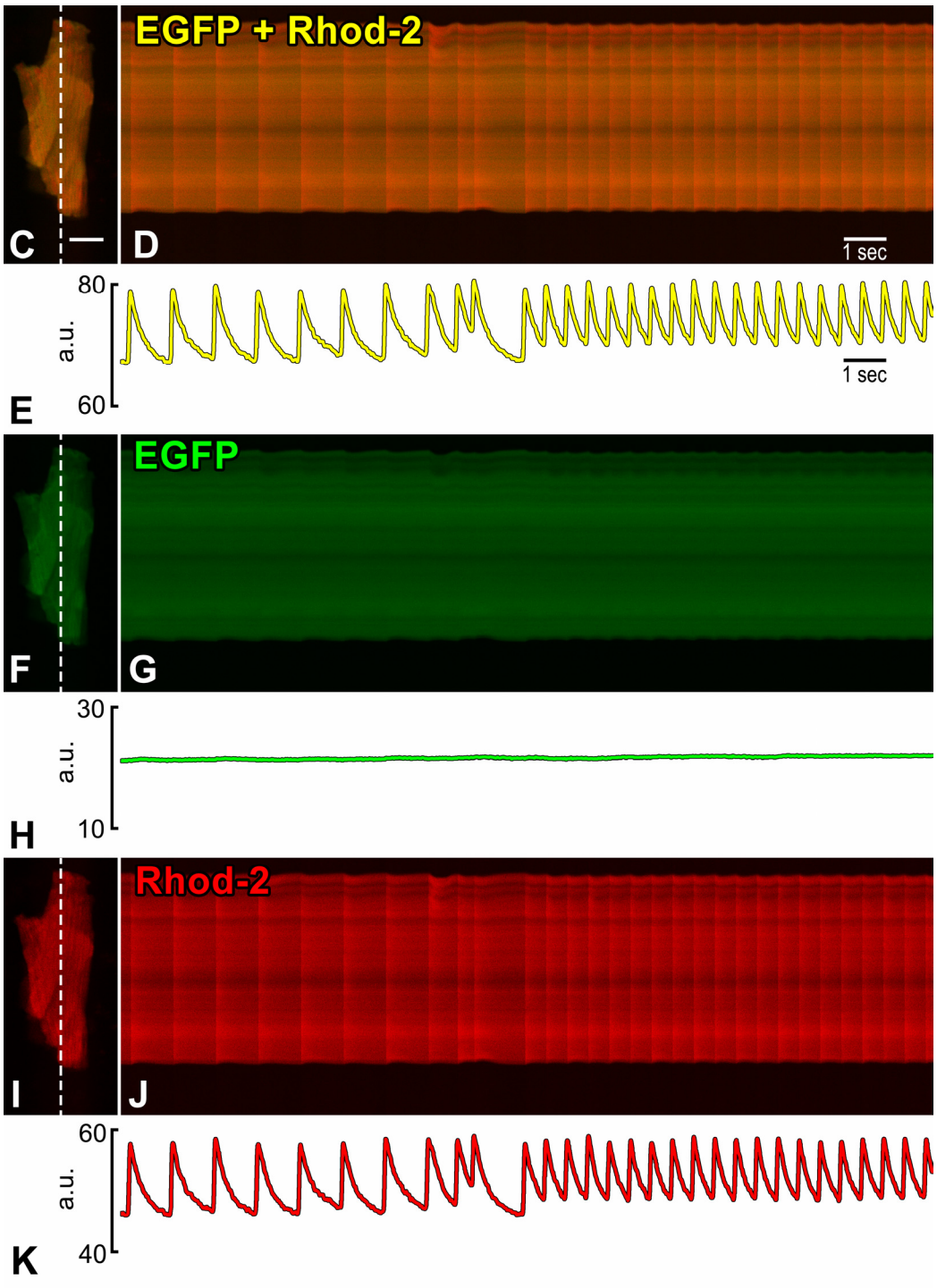

Figure VI. (Continued).

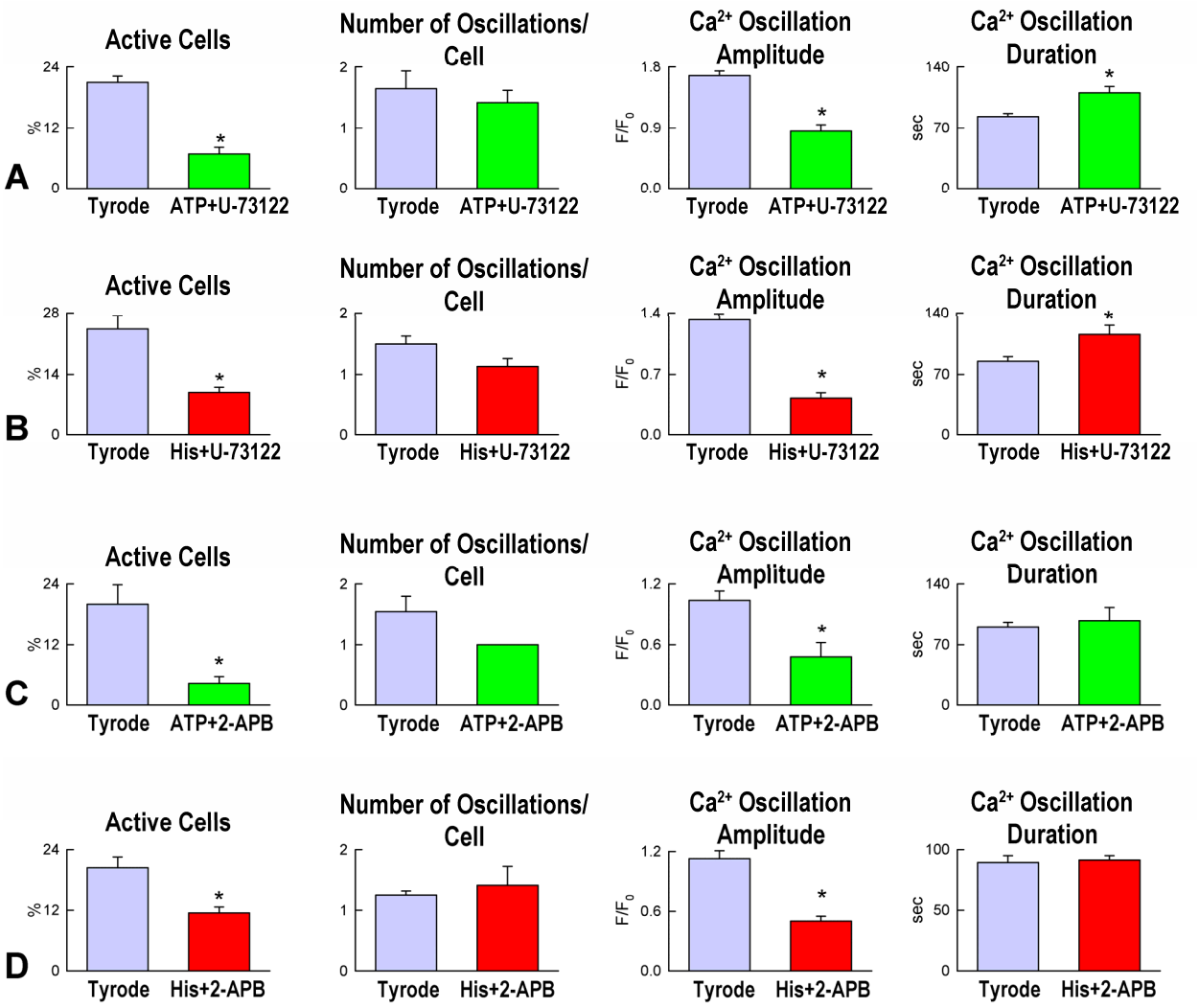

Figure VII. Inhibition of the IP3-IP3R system abrogates the effect of G_q-protein coupled receptors on Ca^{2+} oscillations. **A-D**, Ca^{2+} oscillations at baseline and after exposure to ATP or histamine (His) together with PLC inhibitors (**A** and **B**) or IP3R blocker (**C** and **D**). Histamine, His. **P*<0.05 vs. Tyrode.

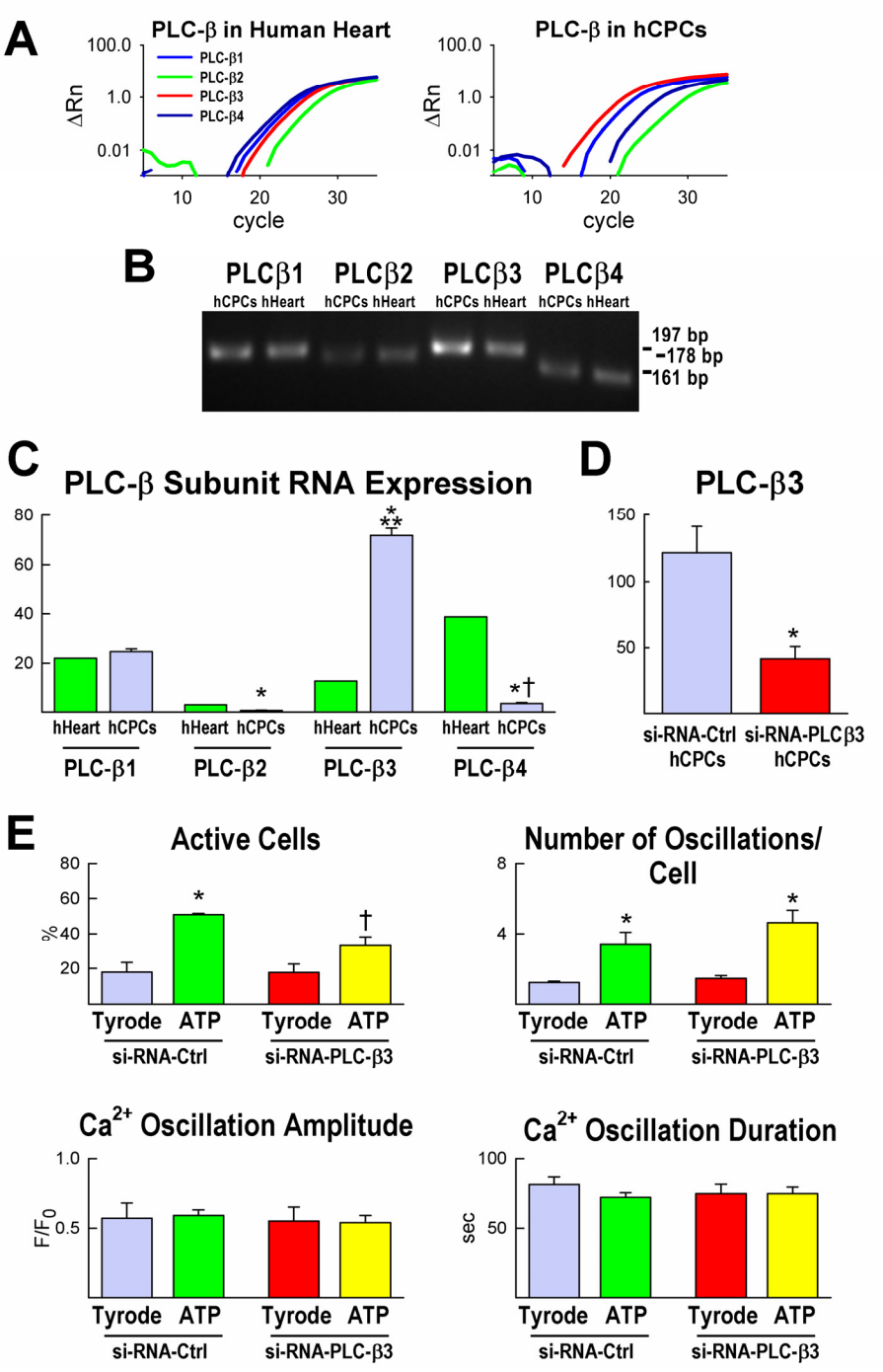

Figure VIII. PLC-β3 and ATP-mediated Ca^{2+} oscillations in hCPCs. **A-C**, Expression at the mRNA of PLC-β subunits in the human heart (hHeart, n=1) and hCPCs (n=3). **D**, PLC-β3 mRNA was significantly reduced in hCPCs transfected with siRNA against human PLC-β3 (si-RNA-PLC-β3, n=3); control hCPCs were transfected with non-targeting siRNA (si-RNA-Ctrl, n=3). **E**, Ca^{2+} oscillations at baseline and after exposure to ATP in si-RNA-Ctr and si-RNA-PLC-β3 hCPCs. **P*<0.05 vs. Tyrode, †*P*<0.05 vs. si-RNA-PLC-β3 cells exposed to ATP.

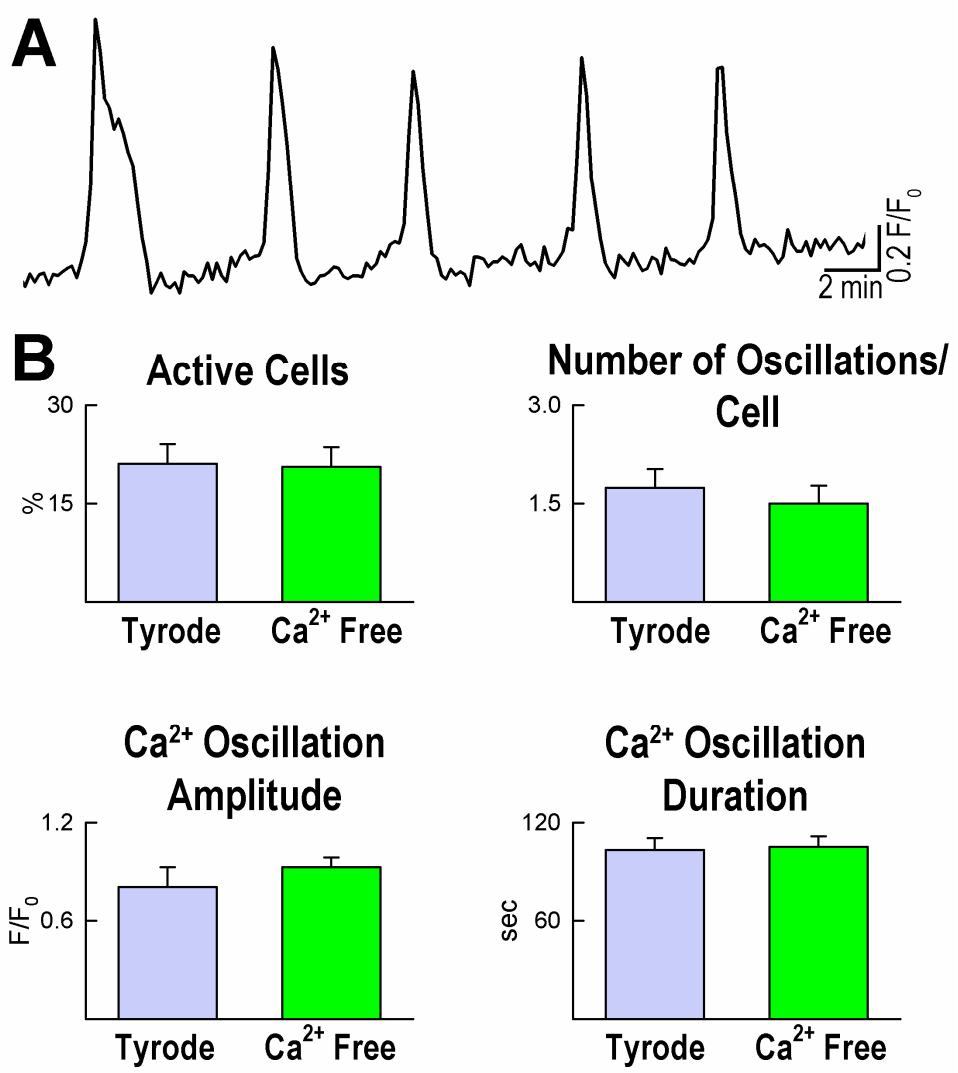

Figure IX. A, Ca^{2+} oscillations in one hCPC exposed to Ca^{2+} free Tyrode solution. **B**, Ca^{2+} oscillations in the presence of 2 mM Ca^{2+} and Ca^{2+} free Tyrode solutions.

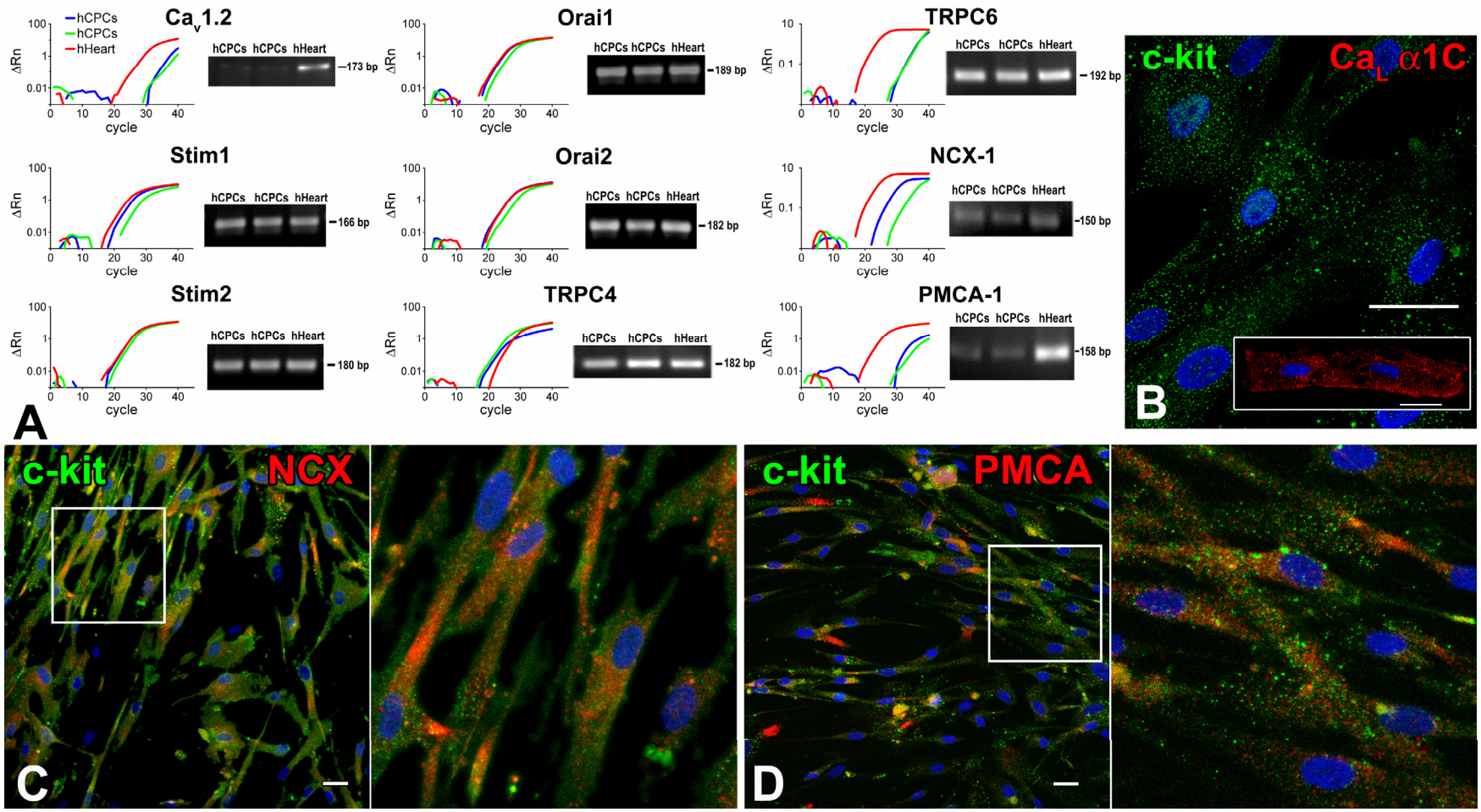

Figure X. Plasma membrane Ca^{2+} regulatory proteins in hCPCs. **A-D**, Expression at the mRNA (**A**) and protein (**B-D**) levels of systems that may be operative in the regulation of $[Ca^{2+}]_i$ in hCPCs; they include the voltage activated L-type channels, store operated channels (SOC), Na^+-Ca^{2+} exchanger (NCX) and plasma membrane Ca^{2+} pump (PMCA). mRNA level of the L-type Ca^{2+} channel subunit $Ca_v1.2$. was low in hCPCs. Transcripts for Stim (stromal interaction molecule), Orai and TRPCs (transient receptor potential channels) which are the putative molecular substrates for SOC (see refs. 17, 35) were present in hCPCs. NCX and PMCA were also identified in hCPCs at the mRNA and protein levels. Myocytes were used as positive control for L-type Ca^{2+} channels. Human heart (hHeart) was used as positive control for mRNA assays. Scale bars: 10 μm.

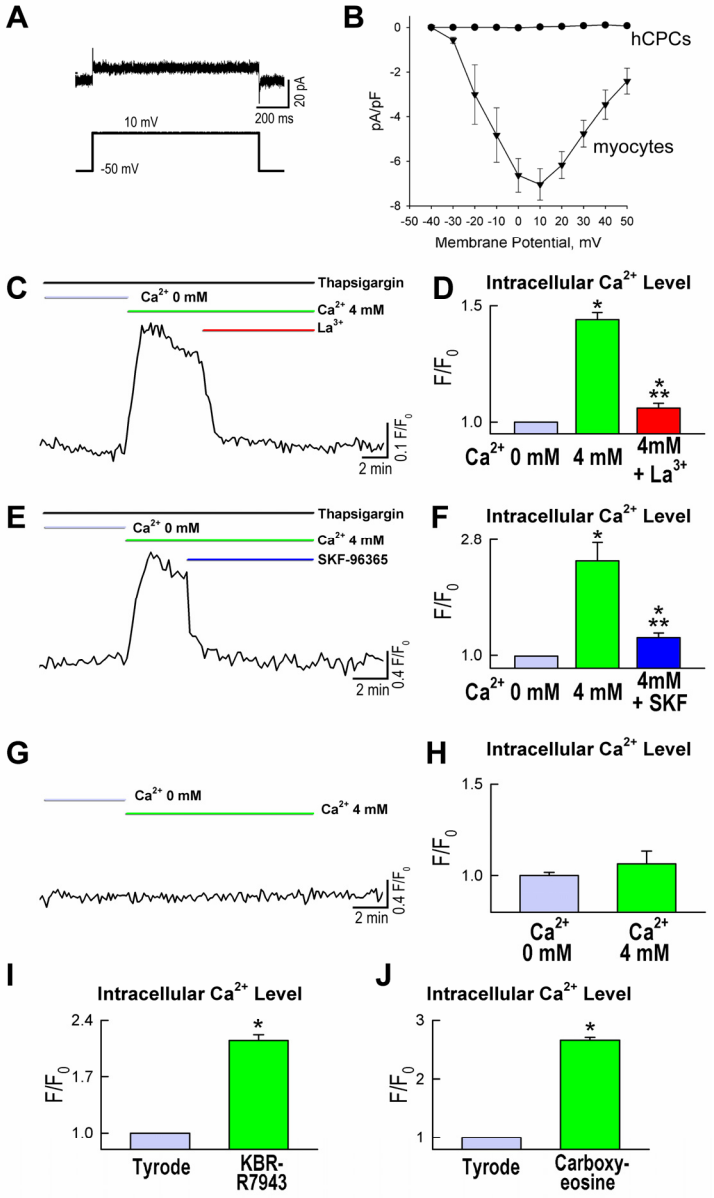

Figure XI. Plasma membrane Ca^{2+} fluxes in hCPCs. **A** and **B**, L-type Ca^{2+} current (I_{CaL}) in hCPCs. Adult mouse myocytes were used as control for this analysis. Depolarizing steps in voltage clamp mode documented the absence of time-dependent voltage activated inward currents at -20 to +50 mV in hCPCs. This corresponds to the range of membrane potentials activating I_{CaL}. A depolarizing step to +10 mV applied to an hCPC is illustrated (**A**). Conversely, I_{CaL} was clearly present in cardiomyocytes as shown by the current-voltage relations for the two cell types (**B**). These results reflected the modest degree of expression of L-type channel subunit $Ca_v1.2$ in hCPCs. **C-F**, The role of SOC in hCPCs was evaluated by monitoring $[Ca^{2+}]_i$ and evoking the current by depleting the ER Ca^{2+} with thapsigargin (SERCA inhibitor) and rapid increase in extracellular Ca^{2+} from 0 to 4 mM (see refs. 4, 11, 17). The parallel increase in intracellular Ca^{2+} was inhibited by La^{3+} or SKF-96365, blockers of SOC (see refs. 4, 11, 17-20). **G** and **H**, SOC was not activated by the increase in extracellular $[Ca^{2+}]$ when SERCA function and Ca^{2+} stores were not depleted. **P*<0.05 vs. Ca^{2+} 0 mM, ***P*<0.05 vs. Ca^{2+} 4 mM. **I**, In a comparable manner, the function of NCX in hCPCs was assessed by blocking forward mode NCX and, thereby, Ca^{2+} extrusion (see refs. 20, 21). This protocol resulted in an increase in cytosolic Ca^{2+}. **P*<0.05 vs. Tyrode. **J**, Similar findings were obtained when the effects of PMCA on Ca^{2+} extrusion were abrogated (see refs. 21, 22).**P*<0.05 vs. Tyrode.

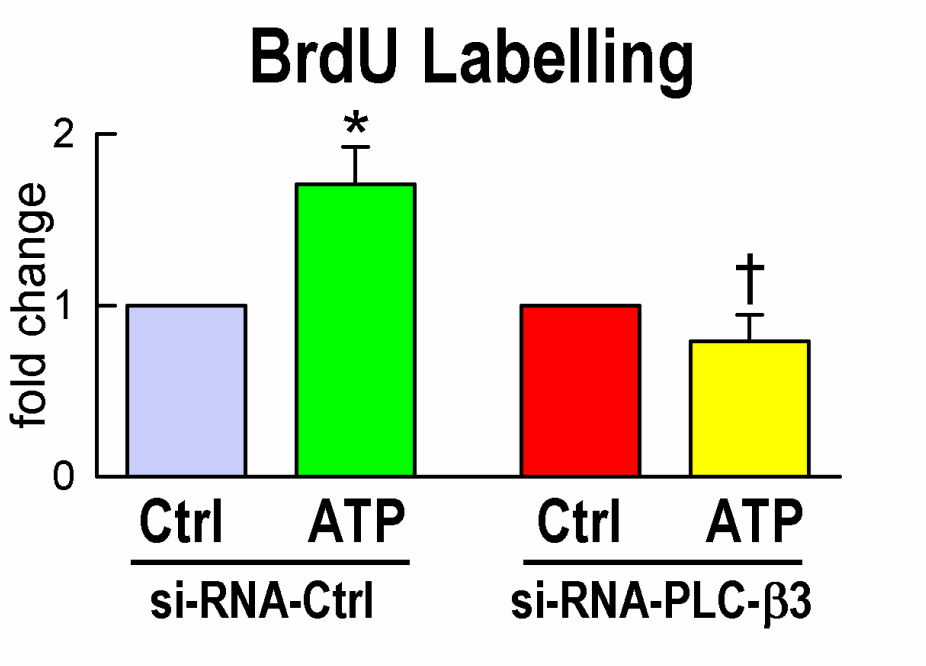

Figure XII. PLC-β3, ATP and hCPC proliferation. Stimulation of hCPC growth by ATP was inhibited after downregulation of PLC-β3 subunit. **P*<0.05 vs. Ctrl, †*P*<0.05 vs. si-RNA-PLC-β3 cells exposed to ATP.

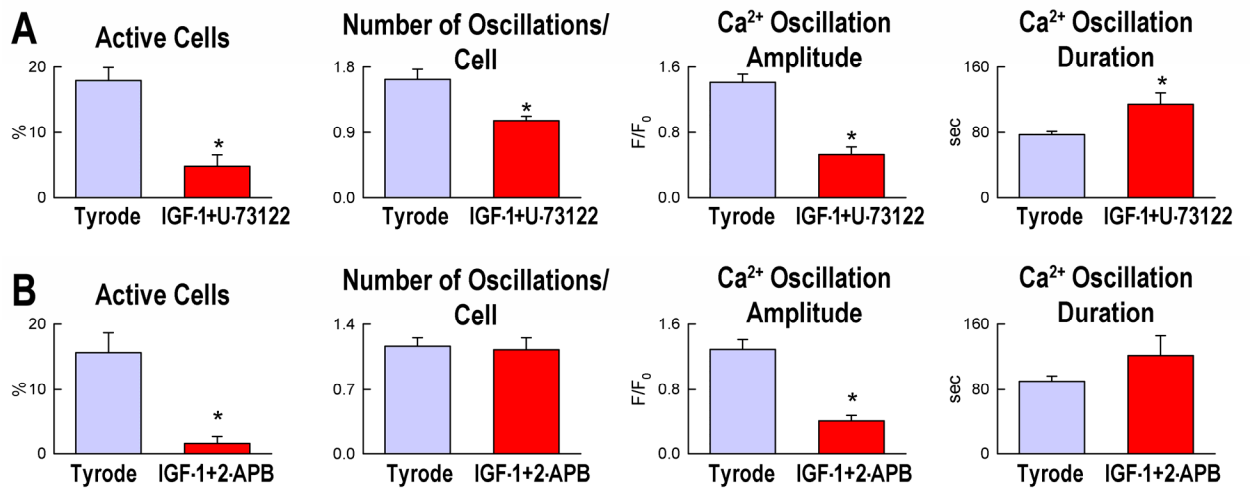

Figure XIII. Inhibition of the IP3-IP3R system abrogates the effect of IGF-1 on Ca^{2+} oscillations. **A** and **B**, Ca^{2+} oscillations in hCPCs at baseline and after exposure to IGF-1 together with inhibition of PLC (**A**) or IP3R (**B**). **P*<0.05 vs. Tyrode.

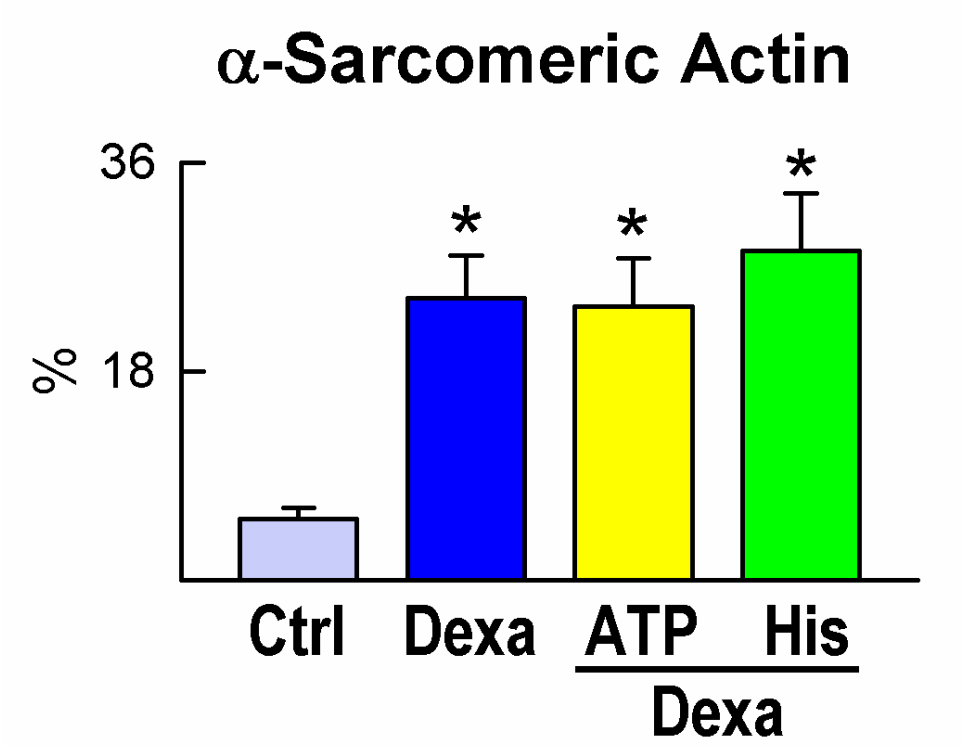

Figure XIV. Ca^{2+} oscillations and hCPC differentiation. Expression of the myocyte-specific cytoplasmic protein α-sarcomeric actin in hCPCs exposed to differentiating medium (dexametasone, Dexa) alone or in combination with modulators of Ca^{2+} oscillations over a period of 7 days. Cells not exposed to differentiating medium were employed as control (Ctrl). Ctrl, n=12; Dexa, n=12; Dexa + ATP, n=12; Dexa + Histamine, n=12. **P*<0.05 vs. Ctrl.

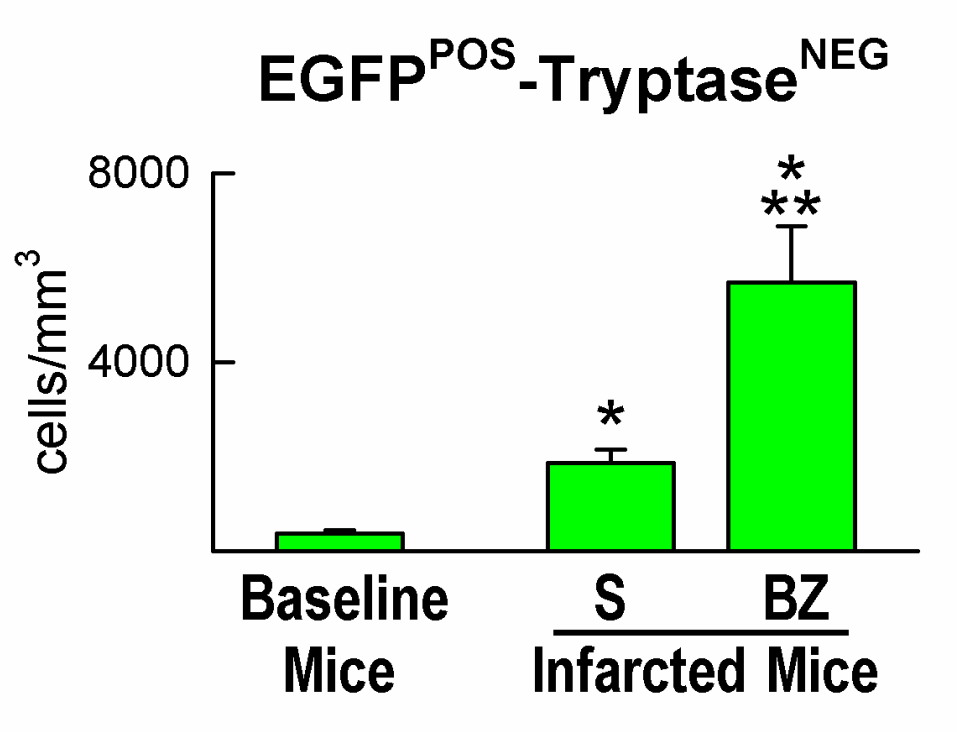

Figure XV. Activation of c-kit-positive CPCs after myocardial infarction. For this analysis transgenic mice expressing EGFP under the c-kit promoter were employed. Number of EGFP-positive in the mouse heart at baseline (n=5) and 2 days after myocardial infarction (n=8) in the surviving (S) distant myocardium and in the border zone (BZ). Because of the ongoing inflammatory reaction in the injured myocardium, tryptase staining was performed to exclude mast cells in the computation.

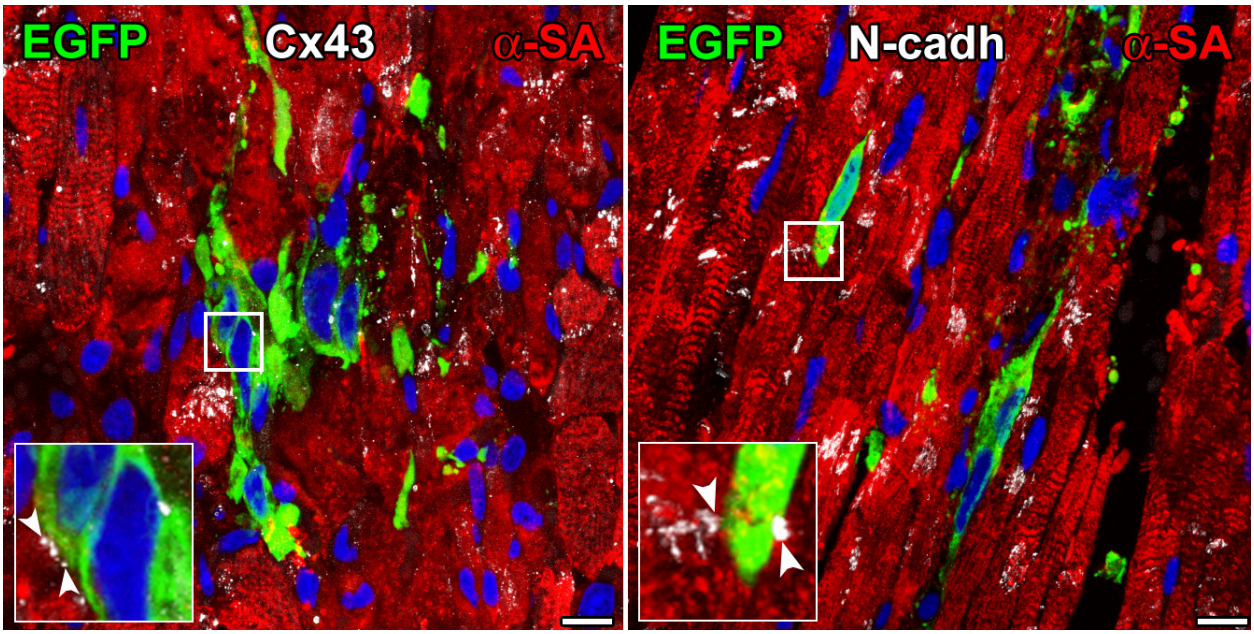

Figure XVI. hCPC engraftment. EGFP-positive hCPCs (EGFP, green) 48 hours after implantation in the infarcted mouse heart express connexin 43 (Cx43, white, left panel) and N-cadherin (N-cadh, white, right panel) at their interface with resident spared myocytes (α-SA, red). Insets show higher magnifications of selected areas. Arrowheads indicate Cx43 (left panel) and N-cadh (right panel) between hCPCs and myocytes. Scale bars: 10 μm.

Supplemental Table 1. Magnitude of sampling for intracellular Ca^{2+} imaging

Cell type	Experimental condition	Number of tests	Number of cells	Number of Ca^{2+} oscillations	Figure
hCPCs	Tyrode	95	3676	1056	1B and 1C
hCPCs	Tyrode	5	101	n/a	1D
Non-synchronized hCPCs (Ctrl)	Tyrode	17	880	n/a	1E
G_1-S synchronized hCPCs	Tyrode	11	453	n/a	
G_2-M synchronized hCPCs	Tyrode	13	770	n/a	
hCPCs	Baseline (Tyrode)	3	102	22	2G
	Octanol		101	31	
Neonatal myocytes	Co-culture: No Stimulation, Electrical Stimulation, Cadmium	3	9, 5, 6	n/a	3B, C
Adjacent hCPCs			14, 12, 8	n/a	
hCPCs	Tyrode	5	165	61	3E
mCPCs		5	186	41	
$EGFP^{POS}$-CPCs, Myocytes (ex vivo)	Tyrode	6 transgenic mice hearts	8 fields with the two cell categories and line-scan recording	n/a	3F

hCPCs	Baseline (Tyrode)	6	261	89	4F
	Thimerosal		427	1493	
hCPCs	Baseline (Tyrode)	7	259	52	4G
	2-APB		257	6	
hCPCs	Baseline (Tyrode)	7	166	73	4G
	Xestospongin-C		149	26	
hCPCs	Baseline (Tyrode)	6	321	121	4H
	U-73122		405	30	
hCPCs	Baseline (Tyrode)	5	264	144	4J
	CPA		212	36	
hCPCs	Baseline (Tyrode)	5	92	27	4L
	Ryanodine		128	31	
hCPCs	Baseline (Tyrode)	6	254	47	4M
	Caffeine		255	48	
hCPCs	Baseline (Tyrode)	6	254	51	5E
	ATP		283	368	
hCPCs	Baseline (Tyrode)	6	300	100	5G
	Histamine		361	793	
hCPCs	Baseline (Tyrode)	5	217	55	7I
	IGF-1		252	187	
hCPCs	Baseline (Tyrode)	4	328	114	Supplemental Figure VII-A
	ATP+U-73122		303	26	
hCPCs	Baseline (Tyrode)	3	171	64	Supplemental Figure VII-B
	Histamine+U-73122		201	15	
hCPCs	Baseline (Tyrode)	5	146	36	Supplemental Figure VII-C
	ATP+2-APB		174	6	
hCPCs	Baseline (Tyrode)	6	259	48	Supplemental Figure VII-D
	Histamine+2-APB		309	48	

si-RNA-Ctrl hCPCs	Baseline (Tyrode)	3	207	19	Supplemental Figure VIII-D
	ATP		226	94	
si-RNA-PLC-β3 hCPCs	Baseline (Tyrode)	3	205	21	
	ATP		197	64	
hCPCs	Baseline (Tyrode)	7	105	23	Supplemental Figure IX-B
	Ca^{2+} free		111	38	
hCPCs	Lanthanum	2	70	n/a	Supplemental Figure XI-D
hCPCs	SKF-96365	2	8	n/a	Supplemental Figure XI-F
hCPCs	Ca2+ 0-4 mM	2	33	n/a	Supplemental Figure XI-H
hCPCs	KB-R7943	4	79	n/a	Supplemental Figure XI-I
hCPCs	Carboxyeosine	3	206	n/a	Supplemental Figure XI-J
hCPCs	Baseline (Tyrode)	5	242	57	Supplemental Figure XIII-A
	IGF-1+U-73122		254	11	
hCPCs	Baseline (Tyrode)	6	185	26	Supplemental Figure XIII-B
	IGF-1+2-APB		224	6	

Supplemental Table 2. Magnitude of sampling for dye transfer experiments

Cell Type	Number of cells	Figure
DiI^{POS} hCPCs	18	Supplemental Figure IV-C
Adjacent DiI^{NEG} hCPCs	29	
Distant DiI^{NEG} hCPCs	52	
DiI^{POS} hCPCs	17	Supplemental Figure V-C
Adjacent DiI^{NEG} Myocytes	16	
Distant DiI^{NEG} Myocytes	32	

Supplemental Table 3. Magnitude of sampling for patch-clamp experiments

Cell Type	Number of cells	Figure
hCPCs	8	6F
Mouse myocytes	6	

Supplemental Table 4. Magnitude of sampling for proliferation assay

Cell type	Experimental condition	Number of tests	Figure
hCPCs	Ctrl	8	6A
	ATP	8	
	ATP + 2-APB	4	
	ATP + U-73122	5	
hCPCs	Ctrl	10	6B
	Histamine	10	
	Histamine + 2-APB	3	
	Histamine + U-73122	3	

hCPCs	Ctrl	6	6C
	2-APB	6	
	Xestospongin-C	3	
	U-73122	6	
hCPCs	Ctrl	12	6J
	IGF-1	12	
	IGF-1 + 2-APB	3	
	IGF-1 + U-73122	4	
si-RNA-Ctrl hCPCs	Ctrl	3	Supplemental Figure XII
	ATP	3	
si-RNA-PLC-β3 hCPCs	Ctrl	5	
	ATP	5	

Supplemental Table 5. Magnitude of sampling for apoptosis assay

Cell type	**Experimental condition**	**Number of tests**	**Figure**
hCPCs	Ctrl	3	6E
	ATP	3	
	Histamine	3	
	2-APB	3	
	U-73122	3	

Supplemental Table 6. Magnitude of sampling for implanted cells

Parameter	Group	Number of animals	Aggregate sample size	Sample size (mean±SD)	Figure
BrdU incorporation	Control	5	707 cells	141±73	7C
	ATP	5	1,711 cells	342±68	
	Histamine	4	1,683 cells	421±57	
Nkx2.5 expression	Control	5	562 cells	112±36	7C
	ATP	5	678 cells	136±74	
	Histamine	4	1,037 cells	207±94	
Myocardial Regeneration	MI+Ctrl-hCPCs	8			8B
	MI+ATP/His-hCPCs	9 (ATP, 7; His, 8)			
Myocyte Volume	MI+Ctrl-hCPCs	8	102		8B
	MI+ATP/His-hCPCs	9 (ATP, 7; His, 8)	207		
LV Hemodynamics	SO	7	n/a	n/a	8C
	MI+PBS	7	n/a	n/a	
	MI+Ctrl-hCPCs	8	n/a	n/a	
	MI+ATP-hCPCs MI+His-hCPCs	9 (ATP, 4; His, 5)	n/a	n/a	

Supplemental Table 7. Antibodies for immunocytochemistry and immunohistochemistry

Protein	**Antibody**	**Detection labelling technique**	**Company**
c-kit	rabbit polyclonal	Indirect (FITC, Cy5)	Santa Cruz
c-kit	goat polyclonal	Indirect (TRITC, Cy5)	R&D Systems
Connexin 43	rabbit polyclonal	Indirect (TRITC, Cy5)	Sigma
IP3R-I/II/III	rabbit polyclonal	Indirect (TRITC, Cy5)	Santa Cruz
RyR	mouse monoclonal	Indirect (FITC, Cy5)	Sigma
SERCA2	goat polyclonal	Indirect (Cy5)	Santa Cruz
NCX	rabbit polyclonal	Indirect (Cy5)	Santa Cruz
PMCA	mouse monoclonal	Indirect (Cy5)	Sigma
P2Y2	rabbit polyclonal	Indirect (FITC, Cy5)	Santa Cruz
H1 Receptor	rabbit polyclonal	Indirect (Cy5)	Sigma
IGF-1-Rα	rabbit polyclonal	Indirect (TRITC, Cy5)	Santa Cruz
BrdU	mouse monoclonal	Indirect (FITC, TRITC)	Roche
EGFP	rabbit polyclonal	Indirect (FITC, TRITC)	Invitrogen
EGFP	goat polyclonal	Indirect (FITC, TRITC)	Abcam
α-sarcomeric actin	mouse monoclonal	Indirect (FITC, TRITC)	Sigma
Nkx 2.5	goat polyclonal	Indirect (TRITC, Cy5)	Santa Cruz
Tryptase	mouse monoclonal	Indirect (TRITC)	Chemicon
N-cadherin	rabbit polyclonal	Indirect (TRITC)	Santa Cruz
L-type Ca^{2+} α1C	goat polyclonal	Indirect (FITC, Cy5)	Santa Cruz

Supplemental Table 8. Primers used in the real-time RT-PCR for human genes

Gene	Forward primers (5'-3')	Reverse primers (5'-3')
IP3R1	GAAGAGCACATCAAGGAAGAACAC	TGCTGACCAATGACATGGCT
IP3R2	TAGTCCTGGTGAAAGTTAAAGACCC	CAGACTCATGGTCGATTCCAACT
IP3R3	TGTACTTCATTGTGCTGGTCCG	CGAATCTCATTCTGCTCCCC
SERCA2	CCGTGTCACAGATCCAGAAGAT	AGGAAAGGGAAGGGGACATG
RyR2	TACTTCGACACAGTGCCACATGG	GTTTCCGGAAGCAATCCCCT
NCX-1	GCTTTCATTGGAGACCTGGC	GGCGTCTGCATACTGGTCCT
PMCA-1	TACCTGAGGAGGAATTAGCAGAGG	AGCCCCCTGAATGGAACTTC
Ca_v 1.2	CCAGTGAGAAACTCAACAGCAGC	ATCAAGACCGCTTCCACCAG
Orai1	GTGATGAGCCTCAACGAGCAC	CACTGAAGGCGATGAGCAGC
Orai2	GGTCACCTCTAACCACCACTCGGT	TGAAGGCAATCAGCAGCGGC
Stim1	TGACTGACGACGTGGATGAC	CTCATGTGGAGGGAGGACTC
Stim2	CTTCCCCTGATCCAGATATCC	CGAGGCTTAAAGGAGGAGAC
TRPC4	TAGGGAGGCGAGCTGCTGAT	ATCCCAGGACTTCAAAGCGG
TRPC6	AACAGGTTGGGCACAATAAACAAC	TGTCCTGCTTAATTTCCTTCAGTTC
P2Y2	CCCTTGTGGCAGCAGCACTA	GCACGGGTTCCTCACTCATG
H1	AGAAGCAAGCCCTGAGGTCTG	GGCTGGCCATAGTGGTCTTG
IGF-1	CCTCAGACAGGCATCGTGGAT	GCACTCCCTCTACTTGCGTTCTT
PLC-β1	AGCAGCCCTGATCATGGTTC	GCGACATCCGTCAACTTTTG
PLC-β2	CTCCCACATCCAGGAAGTAGTGC	TGCCTCCAGACCCTTCATCC
PLC-β3	ACGAGAGGGAGAAGAAGGAGCTG	AGCCACAAGACGGTCATGCC
PLC-β4	GAGCACACCAGGCTAAGATTTC	GGACTGCTTCATGGCAAGTC
GAPDH	GGTCGGAGTCAACGGATTT	TTCCATTGATGACAAGCTTCC

Supplemental References:

1. Bearzi C, Rota M, Hosoda T, Tillmanns J, Nascimbene A, De Angelis A, Yasuzawa-Amano S, Trofimova I, Siggins RW, Lecapitaine N, Cascapera S, Beltrami AP, D'Alessandro DA, Zias E, Quaini F, Urbanek K, Michler RE, Bolli R, Kajstura J, Leri A, Anversa P. Human cardiac stem cells. *Proc Natl Acad Sci USA*. 2007;104:14068-14073.

2. Beltrami AP, Barlucchi L, Torella D, Baker M, Limana F, Chimenti S, Kasahara H, Rota M, Musso E, Urbanek K, Leri A, Kajstura J, Nadal-Ginard B, Anversa P. Adult cardiac stem cells are multipotent and support myocardial regeneration. *Cell*. 2003;114:763-776.

3. Hung DT, Jamison TF, Schreiber SL. Understanding and controlling the cell cycle with natural products. *Chem Biol.* 1996;3:623-639.

4. Kapur N, Mignery GA, Banach K. Cell cycle-dependent calcium oscillations in mouse embryonic stem cells. *Am J Physiol Cell Physiol.* 2007;292:C1510-C1518.

5. Kawano S, Otsu K, Kuruma A, Shoji S, Yanagida E, Muto Y, Yoshikawa F, Hirayama Y, Mikoshiba K, Furuichi T. ATP autocrine/paracrine signaling induces calcium oscillations and NFAT activation in human mesenchymal stem cells. *Cell Calcium*. 2006;39:313-324.

6. Huettner JE, Lu A, Qu Y, Wu Y, Kim M, McDonald JW. Gap junctions and connexon hemichannels in human embryonic stem cells. *Stem Cells*. 2006;24:1654-1667.

7. Bootman MD, Taylor CW, Berridge MJ. The thiol reagent, thimerosal, evokes Ca^{2+} spikes in HeLa cells by sensitizing the inositol 1,4,5-trisphosphate receptor. *J Biol Chem*. 1992;267:25113-25119.

8. Gafni J, Munsch JA, Lam TH, Catlin MC, Costa LG, Molinski TF, Pessah IN. Xestospongins: potent membrane permeable blockers of the inositol 1,4,5-trisphosphate receptor. *Neuron.* 1997;19:723-733.

9. Wu J, Kamimura N, Takeo T, Suga S, Wakui M, Maruyama T, Mikoshiba K. 2-Aminoethoxydiphenyl borate modulates kinetics of intracellular Ca(2+) signals mediated by inositol 1,4,5-trisphosphate-sensitive Ca(2+) stores in single pancreatic acinar cells of mouse. *Mol Pharmacol*. 2000;58:1368-1374.

10. Seidler NW, Jona I, Vegh M, Martonosi A. Cyclopiazonic acid is a specific inhibitor of the Ca2+-ATPase of sarcoplasmic reticulum. *J Biol Chem*. 1989;264:17816-17823.

11. Kawano S, Shoji S, Ichinose S, Yamagata K, Tagami M, Hiraoka M. Characterization of Ca(2+) signaling pathways in human mesenchymal stem cells. *Cell Calcium*. 2002;32:165-174.

12. Smith RJ, Sam LM, Justen JM, Bundy GL, Bala GA, Bleasdale JE. Receptor-coupled signal transduction in human polymorphonuclear neutrophils: effects of a novel inhibitor of phospholipase C-dependent processes on cell responsiveness. *J Pharmacol Exp Ther*. 1990;253:688-697.

13. Kapur N, Banach K. Inositol-1,4,5-trisphosphate-mediated spontaneous activity in mouse embryonic stem cell-derived cardiomyocytes. *J Physiol*. 2007;581:1113-1127.

14. Rota M, Boni A, Urbanek K, Padin-Iruegas ME, Kajstura TJ, Fiore G, Kubo H, Sonnenblick EH, Musso E, Houser SR, Leri A, Sussman MA, Anversa P. Nuclear targeting of Akt enhances ventricular function and myocyte contractility. *Circ Res*. 2005;97:1332-1341.

15. Catanzaro JN, Nett MP, Rota M, Vassalle M. On the mechanisms underlying diastolic voltage oscillations in the sinoatrial node. *J Electrocardiol*. 2006;39:342.

16. Rota M, Hosoda T, De Angelis A, Arcarese ML, Esposito G, Rizzi R, Tillmanns J, Tugal D, Musso E, Rimoldi O, Bearzi C, Urbanek K, Anversa P, Leri A, Kajstura J. The young mouse heart is composed of myocytes heterogeneous in age and function. *Circ Res*. 2007;101:387-399.

17. Parekh AB, Putney JW Jr. Store-operated calcium channels. *Physiol Rev*. 2005;85:757-810.

18. Harper JL, Shin Y, Daly JW. Loperamide: a positive modulator for store-operated calcium channels? *Proc Natl Acad Sci USA*. 1997;94:14912-14917.

19. Hunton DL, Lucchesi PA, Pang Y, Cheng X, Dell'Italia LJ, Marchase RB. Capacitative calcium entry contributes to nuclear factor of activated T-cells nuclear translocation and hypertrophy in cardiomyocytes. *J Biol Chem*. 2002;277:14266-14273.

20. Yanagida E, Shoji S, Hirayama Y, Yoshikawa F, Otsu K, Uematsu H, Hiraoka M, Furuichi T, Kawano S. Functional expression of Ca2+ signaling pathways in mouse embryonic stem cells. *Cell Calcium*. 2004;36:135-146.

21. Iwamoto T, Watano T, Shigekawa M. A novel isothiourea derivative selectively inhibits the reverse mode of Na+/Ca2+ exchange in cells expressing NCX1. *J Biol Chem*. 1996;271:22391-22397.

22. Wanaverbecq N, Marsh SJ, Al-Qatari M, Brown DA. The plasma membrane calcium-ATPase as a major mechanism for intracellular calcium regulation in neurones from the rat superior cervical ganglion. *J Physiol*. 2003;550:83-101.

23. Urbanek K, Cesselli D, Rota M, Nascimbene A, De Angelis A, Hosoda T, Bearzi C, Boni A, Bolli R, Kajstura J, Anversa P, Leri A. Stem cell niches in the adult mouse heart. *Proc Natl Acad Sci USA*. 2006;103:9226-9231.

24. Rota M, Kajstura J, Hosoda T, Bearzi C, Vitale S, Esposito G, Iaffaldano G, Padin-Iruegas ME, Gonzalez A, Rizzi R, Small N, Muraski J, Alvarez R, Chen X, Urbanek K, Bolli R, Houser SR, Leri A, Sussman MA, Anversa P. Bone marrow cells adopt the cardiomyogenic fate in vivo. *Proc Natl Acad Sci USA*. 2007;104:17783-17788.

25. Bevilacqua A, Loch-Caruso R, Erickson RP. Abnormal development and dye coupling produced by antisense RNA to gap junction protein in mouse preimplantation embryos. *Proc Natl Acad Sci USA.* 1989;86:5444-5448.

26. Short AD, Taylor CW. Parathyroid hormone controls the size of the intracellular Ca(2+) stores available to receptors linked to inositol trisphosphate formation. *J Biol Chem.* 2000;275:1807-1813.

27. Cairns LA, Moroni E, Levantini E, Giorgetti A, Klinger FG, Ronzoni S, Tatangelo L, Tiveron C, De Felici M, Dolci S, Magli MC, Giglioni B, Ottolenghi S. Kit regulatory elements required for expression in developing hematopoietic and germ cell lineages. *Blood.* 2003;102:3954-3962.

28. Torella D, Rota M, Nurzynska D, Musso E, Monsen A, Shiraishi I, Zias E, Walsh K, Rosenzweig A, Sussman MA, Urbanek K, Nadal-Ginard B, Kajstura J, Anversa P, Leri A. Cardiac stem cell and myocyte aging, heart failure, and insulin-like growth factor-1 overexpression. *Circ Res.* 2004;94:514-524.

29. Rota M, Vassalle M. Patch-clamp analysis in canine cardiac Purkinje cells of a novel sodium component in the pacemaker range. *J Physiol*. 2003;548:147-165.

30. Gonzalez A, Rota M, Nurzynska D, Misao Y, Tillmanns J, Ojaimi C, Padin-Iruegas ME, Müller P, Esposito G, Bearzi C, Vitale S, Dawn B, Sanganalmath SK, Baker M, Hintze TH, Bolli R, Urbanek K, Hosoda T, Anversa P, Kajstura J, Leri A. Activation of cardiac progenitor cells reverses the failing heart senescent phenotype and prolongs lifespan. *Circ Res*. 2008;102:597-606.

31. Kajstura J, Rota M, Whang B, Cascapera S, Hosoda T, Bearzi C, Nurzynska D, Kasahara H, Zias E, Bonafé M, Nadal-Ginard B, Torella D, Nascimbene A, Quaini F, Urbanek K, Leri A, Anversa P. Bone marrow cells differentiate in cardiac cell lineages after infarction independently of cell fusion. *Circ Res.* 2005;96:127-137.

32. Wallenstein S, Zucker CL, Fleiss JL. Some statistical methods useful in circulation research. *Circ Res.* 1980;47:1-9.

33. Berenson ML, Levine DM, Rindskopf D, eds. Applied statistics, a first course. Englewood Cliffs, New Jersey: Prentice-Hal; 1988.

34. Liao Y, Erxleben C, Abramowitz J, Flockerzi V, Zhu MX, Armstrong DL, Birnbaumer L. Functional interactions among Orai1, TRPCs, and STIM1 suggest a STIM-regulated heteromeric Orai/TRPC model for SOCE/Icrac channels. *Proc Natl Acad Sci USA*. 2008;105;2895-2900.

Legend for Video Files

Supplemental Movie 1. Propagation of a Ca^{2+} wave in a myocyte doublet loaded with Fluo-3.